

Numerical Simulation of Seepage Field of Fractured Surrounding Rock of Balang Mountain Tunnel

Qu Meng-fei¹, Xie Qiang¹, He Jian-jun¹, Li Zhao-yang¹
1. Southwest Jiaotong University, Chengdu 610031, China
E-mail: 793147928@qq.com

Abstract: Through the field survey work, the joints characteristics were acquired and then the consecutive joint network was obtained by Monte Carlo method. According to the joint network, the dominant structural plane of rock mass was summarized. The rock formation is the main flow direction of water compared with other joints from joints network. The permeability tensor was calculated by computer program which is self-programmed and then corrected in the light of permeability coefficient got by field water pressure test. The model for numerical simulation was established in the light of measured tunnel profile. The upper boundary is the measured form line and the lower boundary is confirmed by numerical simulation which is 2500m below the tunnel. The numerical simulation results show that seepage flow is greater in the F1 fault, Jiajinshan anticline and Meixing syncline.

Keywords: tunnel; seepage field; Monte Carlo method.

1. Introduction

In the cold region, freezing injury is a serious problem affecting the normal operation of tunnels. Because the temperature is difficult to measure after totally excavating of tunnels and the cost is large. So numerical simulation method is always employed for simulating temperature field of tunnel in order to provide some references for insulating layer design. Generally, temperature field simulation considers heat convection between rock mass and air, the heat transmission between rock mass, water is rarely considered. Recently, several researches are about to add seepage influence into the temperature field^[1-4].

In this thesis, the Balang Mountain tunnel was the study object, the seepage field of it is studied. The seepage field got by numerical simulation method can offer some parameters for temperature field simulation when considering seepage.

2. Brief introduction of the tunnel

The Balang Mountain tunnel is located at Xiaojin county of Sichuan province. The entrance elevation is 3845m and exit elevation is 3852m. The total length of the tunnel is 8808m and depth is 880m. In tunnel site, the average temperature is 1.8°C, from December to January in the following year the average temperature is below -5°C. The tunnel surrounding rock is interbedding of sandstone and shale. There are three large structures in tunnel site, one is F1 fault, the other is Jiajinshan anticline and the last is Meixing syncline.

3. Joint network simulation

The joint network simulation work has several steps.

(1) Field survey

In field survey work, the shape, occurrence (strike, dip direction, dip angle), extension, density and openness of fractures are measured. The figure 1 is the rock mass picture in Balang Mountain site.



Figure1 An overview of the joints in tunnel site

(2) Clustering analysis for joints

In order to analyze the development regulations of joints, firstly, the joints are grouping by occurrence and then statically by grouping. Generally, the rose diagram of joint and clustering analysis method are used to group and ensure the dominant orientation.

(3) The probability model for joints

The probability distribution function of each element of joint is usually assumed normal distribution, logarithmic normal distribution, negative exponential distribution and uniform distribution. Based on the clustering analysis result, the parameter (average value, stander deviation et al) of each element of joints are got, so the probability models of each element of joints are established

(4) Monte-Carlo simulation

Based on the data got by above steps, the Monte-Carlo method is used to generate joint network. Generally, the joint space, trace length, dip direction and dip angle are complete to describe the spatial form of joint based on the large data obtained by field survey. The joint space is following negative exponential distribution, trace is following logarithmic normal distribution or negative exponential distribution, dip angle and dip direction are mostly following normal distribution or uniform distribution.

There are three sets of joint in tunnel site. The joint 1 occurrence is $244\sim 286^\circ \angle 35\sim 82^\circ$, space is $0.25\sim 0.85\text{m}$, joint 2 occurrence is $160\sim 185^\circ \angle 48\sim 82^\circ$, space is $0.05\sim 0.2\text{m}$, joint 3 occurrence is $75\sim 100^\circ \angle 52\sim 80^\circ$, space is $0.1\sim 0.5\text{m}$. The occurrence of rock formation is $335\sim 348^\circ \angle 78\sim 79^\circ$, space is $0.2\sim 0.6\text{m}$. According to the clustering analysis, the joint 1 and rock formation are selected as the research section. The statistical result of the joint features is listed in Table 1.

Table 1 Statistical results of joint features

Section orientation ($^\circ$)	AVG of angle ($^\circ$)	standard deviation of angle ($^\circ$)	AVG of trace length (m)	standard deviation of trace length (m)	AVG of fault displacement (m)	standard deviation of fault displacement (m)	AVG of space (m)	standard deviation of space (m)
345	28.6	5.24	3.8	1.12	1.5	0.9	2.35	0.55
	61.5	16.9	4.4	0.84	0.9	0.18	3.15	1.21
	84.6	2.52	8.68	1.35	0.28	0.08	0.56	0.36
256	70	6.37	3.9	1.2	0.3	0.08	1.0	0.79
	24	15.7	4.1	1.36	1.2	1.6	0.4	0.24
	81.4	1.89	8	1.23	0.2	0.05	0.45	0.12

Based on the statistical results, the Monte-Carlo method is applied on simulating joint network. The Figure 2 is the preliminary joints network of tunnel site in 345° and 256° directions.

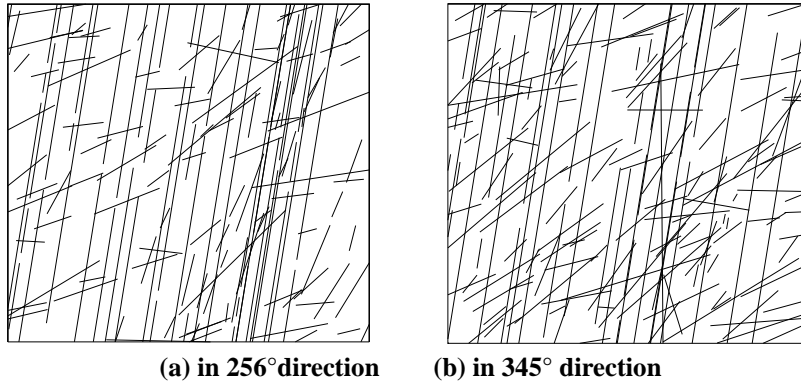


Figure 2 The preliminary joint network of tunnel site

In order to inflect the seepage direction of joints, the above joint network should be handled as consecutive joint network. The Figure 3 is the consecutive joint network of section in 345° and 256° direction which is generated by programming with removing blind fissures. They can reflect the principal direction of hydraulic conductivity of joint plane. We can see that the rock formation is the main flow direction of water compared with other joints from joints network.

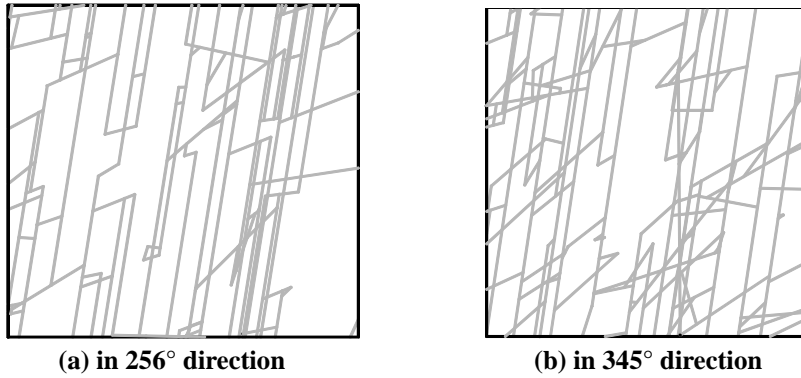


Figure 3 The consecutive joint network

4. Numerical simulation of seepage field of surrounding rock

4.1. Permeability tensor calculation of fissured rock mass

The permeability tensor reflects the permeability anisotropy feature of joint in rock mass, it is the common value which used in representing regularity of water movement in joint.

Assumed in fissured rock mass, there are M sets joints with infinite length. The occurrence, space (b_i), displacement (S_i), angle (α) and inclination (β) of joint is known. In coordinate system, the X direction is the same to North and Y direction is identical with East. The expression of permeability tensor is the equation (1).

$$\bar{K} = \sum_{i=1}^m \frac{rb_i^3}{12vs_i} \begin{bmatrix} K_{xxi} & K_{xyi} & K_{xzi} \\ K_{yzi} & K_{yyi} & K_{yzi} \\ K_{zxi} & K_{zyi} & K_{zzi} \end{bmatrix} \quad (1)$$

Where r : unit weight of water

v : viscosity coefficient of liquid

$$\begin{aligned} K_{xxi} &= 1 - \sin^2 \alpha_i \cos^2 \beta_i \\ K_{xyi} &= K_{yxi} = -\sin^2 \alpha_i \cos \beta_i \sin \beta_i \\ K_{xzi} &= K_{zxi} = -\sin^2 \alpha_i \cos \alpha_i \cos \beta_i \\ K_{yyi} &= 1 - \sin^2 \alpha_i \sin^2 \beta_i \\ K_{yzi} &= K_{zyi} = -\sin \alpha_i \cos \alpha_i \sin \beta_i \\ K_{zzi} &= 1 - \cos^2 \alpha_i = \sin^2 \alpha_i \end{aligned} \quad (2)$$

The data used to calculate permeability tensor is listed in Table 2.

Table 2 Data used for permeability tensor calculating

section	β (°)	α (°)	b (m)	S (m)	viscosity coefficient of water (N·s·m ⁻²)	unit weight of water (N·m ⁻³)
345°	327.2	84.6	10×10^{-4}	0.45	$10^\circ\text{C hour } 1.31 \times 10^{-3}$	9.8×10^3
	250.3	28.6	4×10^{-4}	0.8		
	62.2	61.5	6×10^{-4}	0.9		
256°	330.2	81.4	9×10^{-4}	0.4	$10^\circ\text{C hour } 1.31 \times 10^{-3}$	9.8×10^3
	248.6	24	5×10^{-4}	0.8		
	170	70	4×10^{-4}	0.6		

Using the equation above and field survey data in Table 2, the principal axis and the major permeability coefficient are obtained (Table 3).

Table 3 The calculated result of permeability tensor

section	major permeability coefficient K (cm/s)		azimuth angle (°)	angle (°)	comprehensive permeability coefficient K_0 (cm/s)
345°	K11	4.68×10^{-3}	303.2	88.55	1.30×10^{-3}
	K22	0.74×10^{-3}	211.82	46.08	
	K33	0.63×10^{-3}	34.70	43.95	
256°	K11	8.90×10^{-3}	301.16	87.52	1.80×10^{-3}
	K22	0.93×10^{-3}	208.08	38.96	
	K33	0.71×10^{-3}	33.16	51.15	

The permeability coefficient got by water pressure test is between 0.0857~0.1666m/d, this value is smaller than the calculated value. So, the calculated value must be corrected according to field test. The equivalent permeability coefficient calculated by water pressure test is shown by the following equation:

$$K_\omega = \sqrt[n]{K_1 K_2 \dots K_n} \quad (3)$$

Where K_ω : equivalent permeability coefficient

K_i ($i=1, 2, \dots, n$): Permeability coefficient of every test section

The correction factor:

$$m = K_\omega / K_0 \quad (4)$$

So the corrected permeability tensor K_m is:

$$K_m = mK = \begin{bmatrix} mK_1 & 0 & 0 \\ 0 & mK_2 & 0 \\ 0 & 0 & mK_3 \end{bmatrix} \quad (5)$$

The permeability coefficients calculated by equation 5 are shown in Table 4.

Table 4 The Corrected permeability coefficient

section	K_0 (cm/s)	K_ω (cm/s)	m	K_m (cm/s)
256°	1.80×10^{-3}	1.31×10^{-4}	0.07278	$K_{11} = 3.406 \times 10^{-4}$
				$K_{22} = 5.386 \times 10^{-5}$
				$K_{33} = 4.585 \times 10^{-5}$
345°	1.30×10^{-3}	1.31×10^{-4}	0.10077	$K_{11} = 8.969 \times 10^{-4}$
				$K_{22} = 9.371 \times 10^{-5}$
				$K_{33} = 7.155 \times 10^{-5}$

4.2 The value of parameters for seepage field simulation

The tunnel is divided into 9 parts as the geological conditions. In the light of rainfall intensity provided by meteorological data of tunnel site, every part is assigned different permeability coefficient, as shown in Table 5.

Table 5 Rainfall intensity and permeability coefficient of every part

location	Rainfall intensity ($\text{m}^3/\text{m}^2\cdot\text{s}$)	permeability coefficient(cm/s)
K99+215~99+465	0.034964	0.15
K99+465~99+540	0.001942	0.35
K99+540~99+815	0.00777	0.15
K99+540~100+115	0.003885	0.12
K100+115~100+265 (F1fault)	0.001942	0.35
K100+265~102+265	0.058273	0.12
K102+265~102+415 (Jiajinshan anticline)	0.014139	0.3
K102+415~103+515	0.089351	0.12
K102+415~104+490	0.046618	0.15
K104+490~104+640 (Meixing syncline)	0.058272	0.35
K104+640~105+825	0.027194	0.15
K105+825~107+155	0.097121	0.15

In tunnel site, there are mainly sandstone and shale interbedded, the physical and mechanics parameters of the two type of rock mass are shown in Table 6.

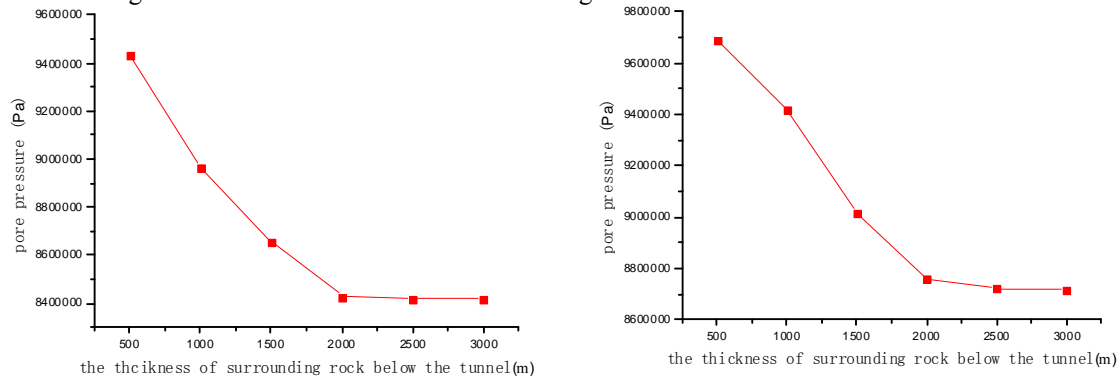
Table 6 Physical and mechanics parameter of rock mass

Rock mass	density (kg/m^3)	Compression modulus (Pa)	shear modulus (Pa)	cohesive force (Pa)	strength of extension (Pa)	internal friction angle ($^\circ$)
shale	2.74e3	4.9e9	1.88e9	1.1e6	7.2e6	28.6
sandstone	2.72e3	9.3e9	4.1e9	5.4e6	9.8e6	42

4.3 The boundary of numerical simulation model

The model for numerical simulation is the same size with Balang Mountain tunnel. The FLAC software is selected as the tool for calculating seepage field of Balang Mountain tunnel.

The upper boundary of the model is the measured form line. The height of lower boundary must be assured by numerical simulation result. In order to make sure that the seepage field will not be affected by model boundary, there are several models of different thicknesses of surrounding rock below the tunnel established. The thicknesses are 500m, 1000m, 1500m, 2000m, 2500m, and 3000m. Compared pore pressures in the same place of different models, when the pore pressure does not change, the thickness is the lower boundary. The Figure 4 is the pore pressure changed with different thicknesses of surrounding rock in 1000m and 2000m from the tunnel entrance.



(a) in the place of 1000m from the tunnel entrance (b) in the place of 2000m from the tunnel entrance

Figure 4 The pore pressure changed with different thickness of surrounding rock below the tunnel

From Figure 4, we can see that when the thickness is over 2000m, the pore pressure is no more changing with surrounding rock thickness in the same place of tunnel. So the lower boundary is ensured which is 2500m height below the tunnel.

4.4 Simulation result of seepage field

The seepage field of totally excavated condition of the tunnel is simulated. The figure 5 and figure 6 are the contour map of water head and the nephogram of pore pressure of seepage field of the tunnel.

Influenced by the different permeability coefficient and form line, the features of seepage field are as follows: in the geology structure of F1 fault, Jiajinshan anticline and Meixing syncline, the prior flow conduit is easily

generated, so the head pressure is lower in these places. Therefore, for this tunnel, according to the seepage field, the water flowing in the crushed zone is larger. When the tunnel is excavated, the places mentioned above should be given more attention.

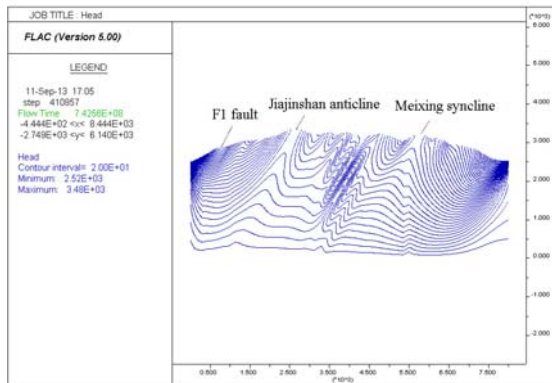


Fig. 5 The contour map of water head

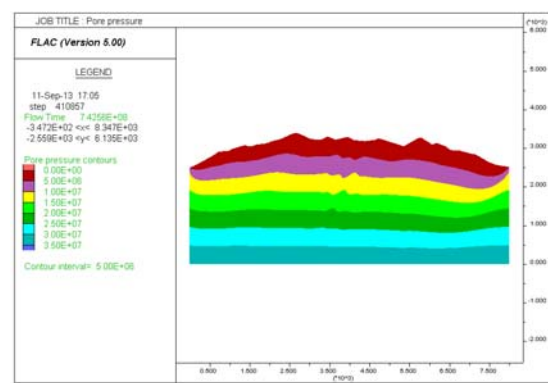


Fig. 6 The nephogram of pore pressure

5. Conclusions

- 1) The main flow direction of water in rock mass is along the rock formation, the penetrating of other set of joints is weak.
- 2) The water discharged in F1 fault, Jiajinshan anticline and Meixing syncline is bigger, when excavating these locations the more attention should be paid.

References

- [1] Jing Shao-dong, Xu Shuai-ling, Wang Chao-guo. Analysis of water-rock interaction and two-dimensional seepage field of tunnel. *Advanced Materials Research*, v 955-959, p 3297-3301.
- [2] Li Chun-lin. Finite element simulation of seepage field and analysis of soil deformation around tunnel due to shield tunneling. *Dongnan Daxue Xuebao*, v 40, n 5, p 1066-1072.
- [3] Huang Tao, Yang Li-zhong. A study of mathematical model on coupling between temperatures. -seepage in fractured rock mass surrounding tunnel. *Chinese Journal of Geotechnical Engineering*, Vol.21 No.5, p554-558.
- [4] Rong Guan, Zhou Chuang-bing, Wang En-zhi. Preliminary study on permeability tensor calculation of fractured rock mass and its representative elementary volume. *Chinese Journal of Geotechnical Engineering*, Vol.26 No .4, p740-746.